Available online at www.sciencedirect.com
ScienceDirect
Ceramics International 37 (2011) 843–849
CERAMICS INTERNATIONAL
www.elsevier.com/locate/ceramint

The hindering function of phosphate on the grain growth behavior of nanosized zirconia powders calcined at high temperatures

Juan Liu [a], Bin Lu [a], Jingze Liu [b], Yanfeng Zhang [a,*], Yu Wei [a]

[a] College of Chemistry and Material Science, Hebei Normal University, Shijiazhuang 050016, China
[b] College of Life Science, Hebei Normal University, Shijiazhuang 050016, China

Received 4 August 2010; received in revised form 16 August 2010; accepted 14 October 2010
Available online 17 November 2010

Abstract

Nanosized zirconia was prepared by a hydrothermal method using $ZrOCl_2 \cdot 8H_2O$ and NaOH as raw materials. The obtained ZrO_2 powders were soaked in the phosphate solution with different concentrations. The as-prepared ZrO_2 powders and the powders treated with phosphate solution were calcined at different temperatures from 600 to 1000 °C. The samples were characterized by X-ray diffraction (XRD), Fourier transform infrared spectroscopy (FTIR), transmission electron microscopy (TEM) and X-ray photoelectronic spectroscopy (XPS). The experimental results show that the untreated nanosized ZrO_2 grow and agglomerate to bulk when the ZrO_2 powders were calcined at high temperatures, while the ZrO_2 powders treated with phosphate solution grow slowly and remain nanosized crystal at the same calcination temperature. This phenomenon implied that phosphate treatment played an important role in inhibiting the crystal grain growth of ZrO_2. The possible inhibition mechanism could be explained to that P species on the surface of ZrO_2 can reduce the grain boundary mobility and prevent direct contact of ZrO_2 particles.

Keywords: Zirconia; Nanosized; Grain growth; Phosphate

1. Introduction

Zirconia ceramic has been a very popular focus of research in materials science and engineering due to its high strength and toughness, good corrosion and abrasion resistance, high melting point, refractory and low thermal conductivity [1–5]. In order to obtain a defect free microstructure in the final ceramic products, the nanosized powders are widely used to fabricate the uniform and dense green bodies. However, particle aggregation is still a particular problem encountered during the sintering process. Therefore, the dispersion and thermal stability of nanosized ZrO_2 particles play a key role in controlling the shape forming behavior and optimizing the performance of the ceramic materials.

In order to achieve full densification, excessive grain growth has to be inhibited either by the incorporation of the second phase particle or solid solution alloy during sintering and high-temperature deformation [6–9]. The high temperature strongly affects the crystal structure, particle size and surface area [10]. Keeping the small particle size can improve the performance of zirconia in many high temperature application fields. In order to optimize the applications in ceramics material, it is essential to investigate the relationship between calcination temperature and grain size. In recent years, the effect of phosphate doping on the nature and property of metal oxides has been widely discussed. Kőrösi et al. indicated that the effect of phosphoric acid treatment on $SnO_2 \cdot nH_2O$ was to inhibit not only the sintering of particles but also the crystal growth of P-SnO_2 during calcinations [11]. Yu et al. found that the incorporation of phosphorus into the inorganic framework of mesoporous TiO_2 from H_3PO_4 can inhibit the grain growth and stabilize the mesoporous structure of TiO_2 [12]. Parida et al. studied the preparation, surface characteristics and acidic sites of phosphated zirconia [13]. In our previous paper, it has been found that phosphate can effectively inhibit the grain growth of nanosized SnO_2 and TiO_2 powders when calcined at high temperatures [14,15]. However, there have been few systematic studies on the effect of phosphate treatment on grain growth of nanosized ZrO_2 when the powders were calcined at high temperatures.

* Corresponding authors. Tel.: +86 0311 86268342; fax: +86 0311 86268342.
E-mail addresses: zhyf@emails.bjut.edu.cn (Y. Zhang), weiyu@mail.hebtu.edu.cn (Y. Wei).

0272-8842/$36.00
doi:10.1016/j.ceramint.2010.10.015

In this work, ZrO_2 powders prepared by a hydrothermal method were soaked in the phosphate solution with different concentrations. And the treated powders were calcined at different temperatures from 600 to 1000 °C. XRD, FTIR, TEM and XPS technologies were used to investigate the inhibition effect of phosphate on the microstructures and grain growth in detail.

2. Experimental procedure

2.1. Materials

An appropriate amount of analytic grade $ZrOCl_2{\cdot}8H_2O$ and NaOH were dissolved in the distilled water respectively. Then the $ZrOCl_2$ solution was added to the NaOH solution. The final concentrations of $ZrOCl_2$ and NaOH in the mixed solution were 0.5 M and 2 M, respectively. Eighty milliliters of the mixed solution was added to a 100 mL Teflon-lined stainless steel autoclave and heated at 200 °C for 5 h. After the autoclave was cooled naturally, the white product obtained was filtered off, washed with distilled water, and then dried at 80 °C for 12 h. Then the powders were calcined at 600 °C for 4 h to obtain zirconia powders. The as-prepared powders were dipped in the NaH_2PO_4 solution with different concentrations for 24 h. Then the powders were filtered, washed with distilled water, and then dried at 80 °C for 12 h. The powders soaked in the phosphate solution are denoted as P-ZrO_2. Then the phosphated zirconia was calcined in a muffle furnace at 600, 800, 900, and 1000 °C for 2 h or 4 h respectively.

2.2. Characterization

The XRD patterns of the obtained samples were examined by X-ray diffraction (XRD) on a Bruker D8 Advance diffractometer with Cu Kα radiation. The crystal grain size was estimated from Scherrer formula as follows:

$$D = \frac{K\lambda}{b\cos q}$$

where D is the crystallite size, λ is the wavelength of the X-ray radiation, K is a constant taken as 0.94, θ is the diffraction angle, and β is the peak width at half-maximum height for $(\bar{1}\,1\,1)$ plane diffraction of zirconia dioxide given by $\beta = \beta_m - \beta_s$, where β_m is the measured half-width and β_s is the half-width of a standard sample. The value of β_m was estimated by the program of Topas P2.1, which is attached in the diffractometer. The morphology of the samples was observed by transmission electron microscopy (TEM) on a Hitachi 7500, using an accelerating voltage of 25 kV. Fourier transform infrared (FTIR) spectroscopy measurement was made with a Japan SHIMADIU FTIR-8900 equipment from 3500 to 500 cm^{-1}, using KBr pellet method. X-ray photoelectron spectroscopy (XPS) measurements were performed in a VG Scientific ESCALAB Mark II spectroscopy to determine the binding state of the Zr, O and P ions. The C (1s) level was used as an internal reference at 284.6 eV.

3. Results and discussion

3.1. XRD analysis

Fig. 1 shows the XRD patterns of the as-prepared sample and the samples calcined at 600, 800, 900, and 1000 °C for 2 h respectively. It can be found that the as-prepared sample was Baddeleyite ZrO_2 (JCPDS, No. 37-1484). With the increase in the calcination temperature the diffraction peaks become sharper and narrower, indicating that the crystal grain of the samples grow larger.

Fig. 2 gives the typical XRD patterns of the as-prepared sample and the samples calcined at 600, 800, 900, and 1000 °C for 4 h respectively. In accordance with the result of the as-prepared sample calcined for 2 h, the diffraction peaks become sharper and narrower with the increasing calcination temperature. Figs. 3 and 4 illustrate the XRD patterns of the as-prepared sample and the samples which were soaked in 0.5 M phosphate solution and calcined at 600, 800, 900, and 1000 °C for 2 h and 4 h respectively. With the increase in the calcination temperature the diffraction peaks of the samples dipped in the phosphate solution remain wider, which indicates the crystal grain of the samples treated by phosphate grow slowly compared with the samples without treatment. Even if the P-ZrO_2 was calcined at high temperature for 4 h, the particle size of samples remains smaller with the increasing calcination temperature. The grain sizes of ZrO_2 samples calculated by Scherrer equation with the XRD data of crystal face (1 1 1) of ZrO_2 are shown in Table 1. Table 1 shows the crystal sizes of ZrO_2 and P-ZrO_2 samples soaked in the phosphate solution with the concentration of 0.1, 0.3, 0.5 and 1.0 M respectively and calcined at different time intervals and calcination temperatures.

For comparison, the grain sizes of ZrO_2 and P-ZrO_2 soaked in phosphate solution with different concentrations, which were calcined at different temperatures for 2 h or 4 h

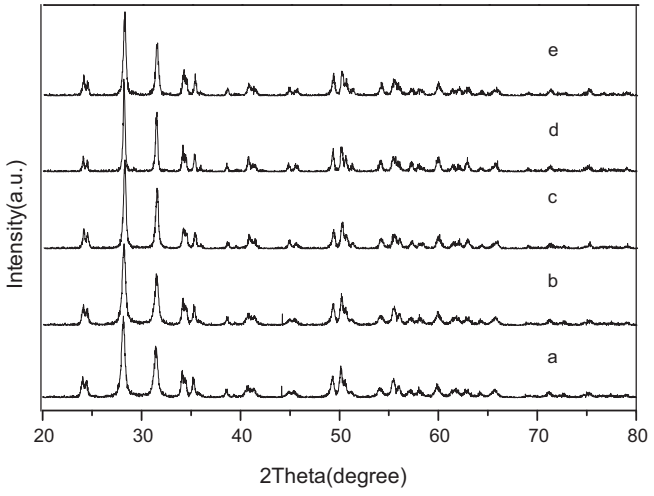

Fig. 1. XRD patterns of the as-prepared samples and the sample calcined at various temperatures for 2 h: (a) as-prepared; (b) 600 °C; (c) 800 °C; (d) 900 °C; (e) 1000 °C.

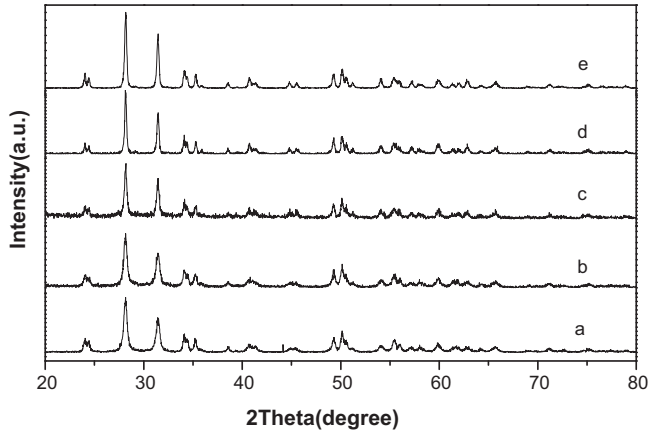

Fig. 2. XRD patterns of the as-prepared sample and the samples calcined at various temperatures for 4 h: (a) as-prepared; (b) 600 °C; (c) 800 °C; (d) 900 °C; (e) 1000 °C.

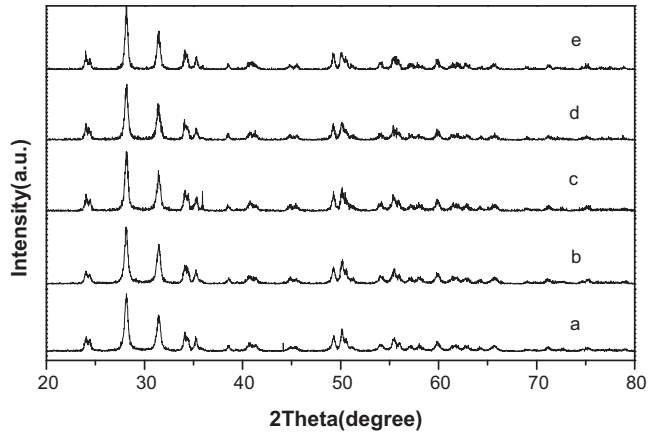

Fig. 3. XRD patterns of (a) as-prepared sample and (b–e) P-ZrO_2 samples soaked in phosphate solution (0.5 M) and calcined at 600, 800, 900 and 1000 °C for 2 h, respectively.

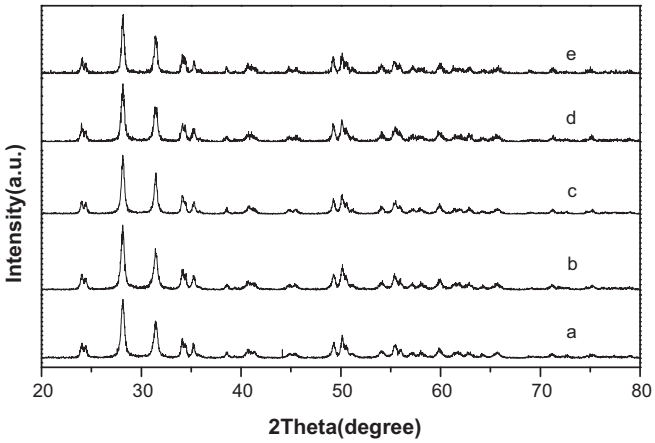

Fig. 4. XRD patterns of (a) as-prepared sample and (b–e) P-ZrO_2 samples soaked in phosphate solution (0.5 M) and calcined at 600, 800, 900 and 1000 °C for 4 h, respectively.

Table 1
Crystal sizes of ZrO_2 and P-ZrO_2 soaked in the phosphate solution with different concentrations and calcined at different time intervals and temperatures.

Time	Temperature	Grain sizes of samples (nm)				
		0 M	0.1 M	0.3 M	0.5 M	1.0 M
2 h	600 °C	27.9	27.0	26.9	26.0	26.7
	800 °C	47.5	34.5	28.6	27.6	27.0
	900 °C	75.4	43.9	40.5	34.6	37.2
	1000 °C	120.0	65.8	57.2	54.8	51.9
4 h	600 °C	29.2	28.3	27.4	26.5	28.4
	800 °C	62.8	36.4	30.7	27.8	30.6
	900 °C	76.0	45.2	44.5	37.4	38.2
	1000 °C	126.0	69.2	61.1	59.2	60.3

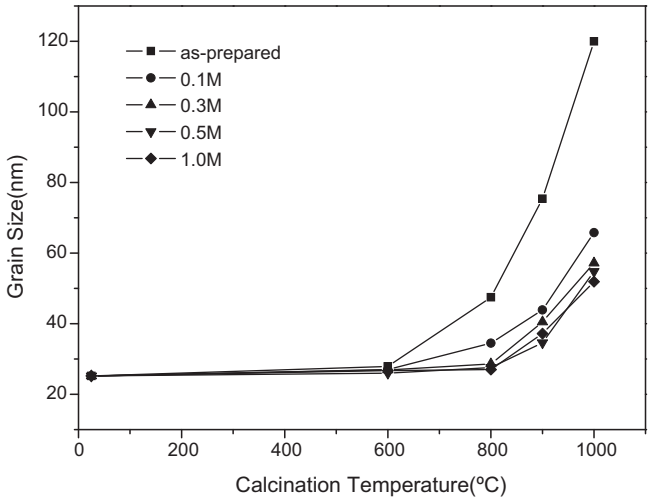

Fig. 5. Relationship between the calcination temperature and grain size of as-prepared samples and the samples, which were soaked in phosphate solution with different concentrations and calcined for 2 h.

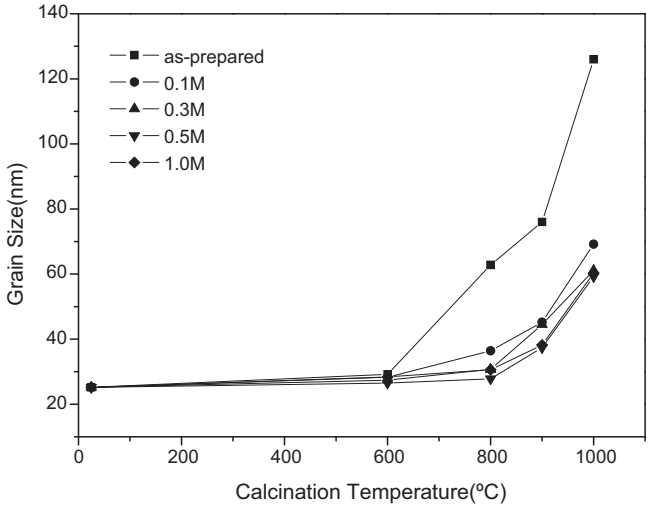

Fig. 6. Relationship between the calcination temperature and grain size of as-prepared samples and the samples, which were soaked in phosphate solution with different concentrations and calcined for 4 h.

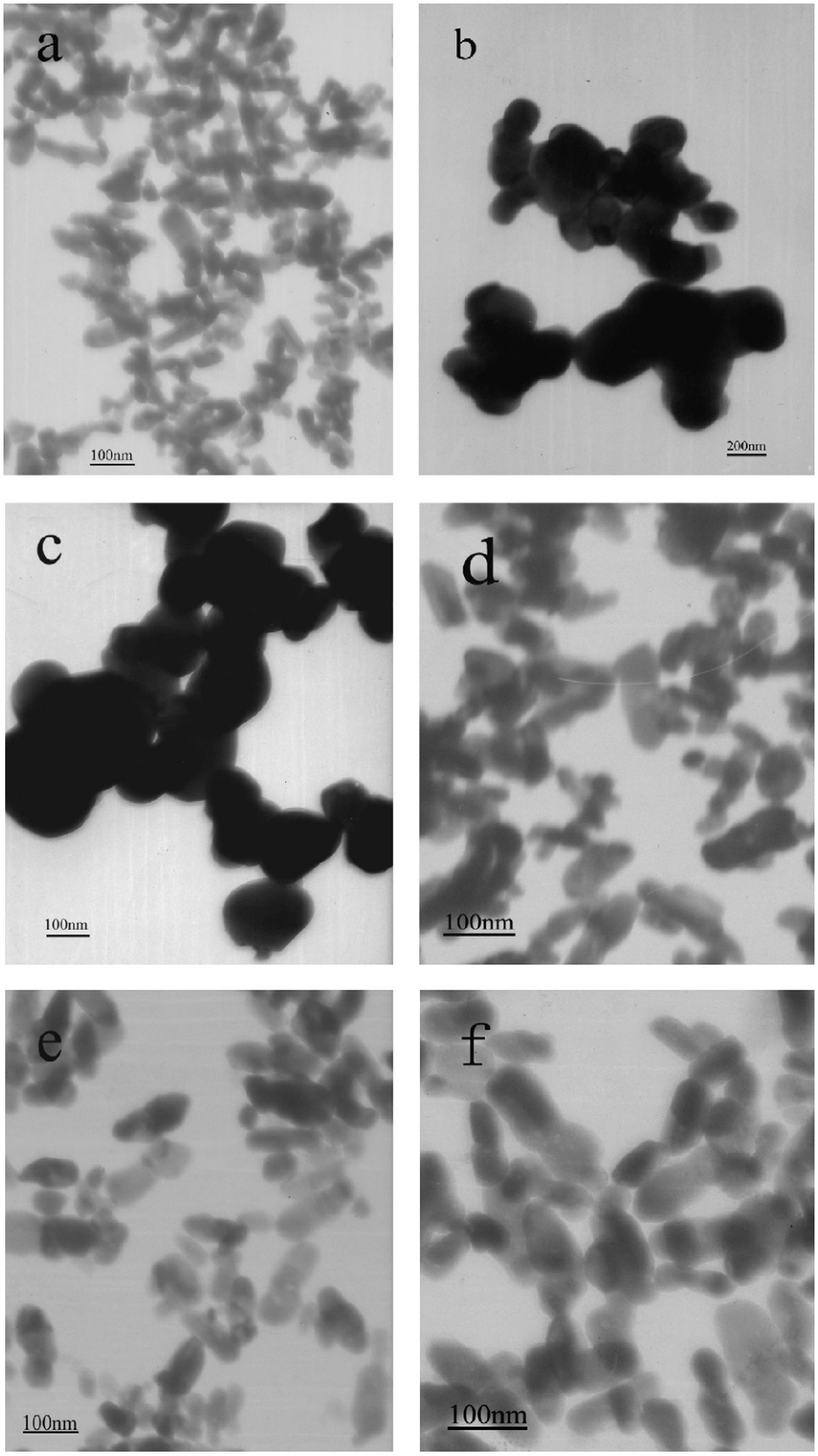

Fig. 7. TEM of the samples: (a) as-prepared; (b) as-prepared sample calcined at 900 °C; (c) as-prepared sample calcined at 1000 °C; (d) P-ZrO_2 calcined at 800 °C; (e) P-ZrO_2 calcined at 900 °C; (f) P-ZrO_2 calcined at 1000 °C.

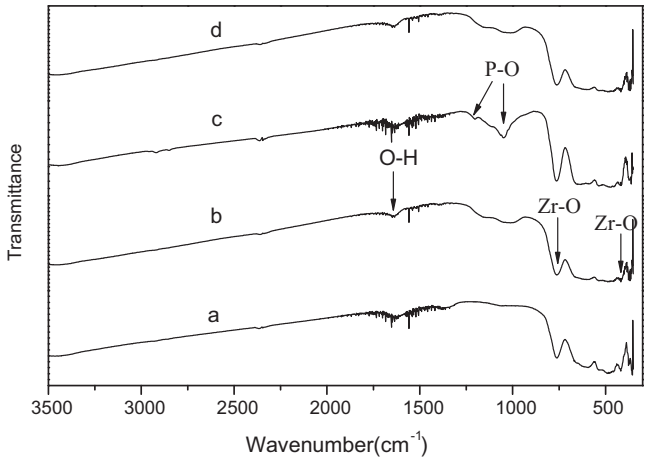

Fig. 8. FTIR spectra of the samples: (a) as-prepared; (b) P-ZrO_2; (c,d) P-ZrO_2 calcined at 900 °C and 1000 °C for 2 h.

respectively, were illustrated in Figs. 5 and 6. It was clearly seen that the crystal grain of the samples without phosphate treatment grows faster than that of the phosphated samples. When the temperature is up to 1000 °C, the average crystal grain of the sample without phosphate treatment is 120 nm (calcined for 2 h) and 126 nm (calcined for 4 h), while the even crystal grain of the P-ZrO_2 is 52 nm (calcined for 2 h) and 60 nm (calcined for 4 h), respectively. It can be deduced that the treatment by the phosphate solution with different concentrations plays an important role in inhibiting the growth of the crystal grain of ZrO_2 and the concentrations of phosphate have no evident difference in the control of the crystal grain growth.

3.2. Particle morphology

The morphology and particle size of the samples were further investigated by TEM. Fig. 7(a–c) shows the morphologies of as-prepared ZrO_2 and the samples calcined at 900 and 1000 °C for 2 h respectively. The as-prepared ZrO_2 powders are rodlike with the average diameter of 26 nm and length of 50 nm. With the increase in calcination temperature, the particles of as-prepared ZrO_2 grow to spherelike and agglomerate to bulk seriously. Fig. 7(d–f) gives the morphologies of P-ZrO_2 which were soaked in 0.5 M phosphate solution and calcined at 800, 900 and 1000 °C respectively. By comparison, it can be obviously seen that the particles of P-ZrO_2 calcined at the same condition remain the original rodlike morphology and grow much smaller than the untreated samples. The images showed that the average diameter of the untreated ZrO_2 calcined at 900 °C and 1000 °C are about 80 nm and 120 nm respectively. While the diameter of P-ZrO_2 samples are with the diameter of 40–50 nm and the length of 100 nm, which is in good accordance with the results calculated by XRD data. From the TEM analysis we can conclude that phosphate treatment plays an important role in inhibiting the grain growth of nanocrystal ZrO_2.

3.3. FTIR spectra

In order to reveal the role of phosphate in inhibiting the grain growth of ZrO_2, FTIR spectra of the as-prepared sample, P-ZrO_2 and P-ZrO_2 calcined at 900 °C and 1000 °C for 2 h were measured as shown in Fig. 8. The absorption band at 1626.3 cm^{-1} is attributed to the stretching mode of O–H bonds in surface adsorption water [16]. The peaks in the region between 1100 and 900 cm^{-1} ascribed to the characteristic peak of phosphate ions, which are absent in the as-prepared sample. The peak at 1053 cm^{-1} is the symmetric stretching of P–O in PO_4^{3-} group [17,18]. The peak at 1099 cm^{-1} is attributed to the antisymmetric stretching of P–O in PO_4^{3-} group. The absorption peaks at 418 and 745 cm^{-1} are of typical monoclinic zirconia, which are in good agreement with the literature [5]. After thermal treatment, the peak induced by physical adsorbtion of phosphate group could be eliminated. The three peaks corresponding to PO_4^{3-} group still remain in the P-ZrO_2 sample even if the P-ZrO_2 sample was calcined at 900 °C and 1000 °C for 2 h respectively. These results imply that phosphate ions are chemically adsorbed on the surface of ZrO_2.

3.4. XPS analysis

To obtain information relative to the chemical states of the ZrO_2 nanoparticles, the typical XPS spectrum of P-ZrO_2 calcined at 800 °C was performed, as shown in Fig. 9(a). The peaks located at 181.33 and 183.73 eV are attributed to the spin–orbit splitting of the Zr 3d components [19]. Meanwhile, the peaks of other elements, including C 1s, O 1s and P 2p were obtained, suggesting PO_4^{3-} ions and ZrO_2 have been successfully assembled in the P-ZrO_2 sample. The P 2p binding energy of P-ZrO_2 is observed at 133.8 eV. This value is in very good agreement with the literature [20].

The high-resolution XPS spectrum of O 1s taken on the surface of P-ZrO_2 calcined at 800 °C for 2 h is shown in Fig. 9(b). The O 1s region of the calcined P-ZrO_2 can be fitted by four peaks, which correspond to Zr–O bonds (530.0 eV), P–O bonds (530.6 eV), hydroxyl groups (531.6 eV), and C–O bonds (532.8 eV), respectively [12,19]. The results further confirm that P–O bond bonds to the surface of zirconia.

Fig. 9(c) illustrates the high-resolution XPS spectra of P 2p taken on the surface of P-ZrO_2 calcined at different temperatures. The peak at around 133.8 eV can be assigned to P 2p binding energy. The binding energy at 133.8 eV indicates that physically and chemically phosphorus exists in the state of pentavalent-oxidation (P^{5+}) and phosphorus species are absorbed on the surface of ZrO_2 [21]. The concentrations of P atom on the surface of ZrO_2 calculated by XPS data are shown in Fig. 9(d). It was found that the atomic ratios of P species on the surface of ZrO_2 slightly decrease with the increasing calcination temperature. The phenomenon could be explained that the small quantity of P atoms physically adsorbed on the surface of ZrO_2 disappear when the P-ZrO_2 samples were calcined at high temperatures.

According to the experimental results of XRD, FTIR, TEM and XPS investigations, the possible mechanism of inhibition

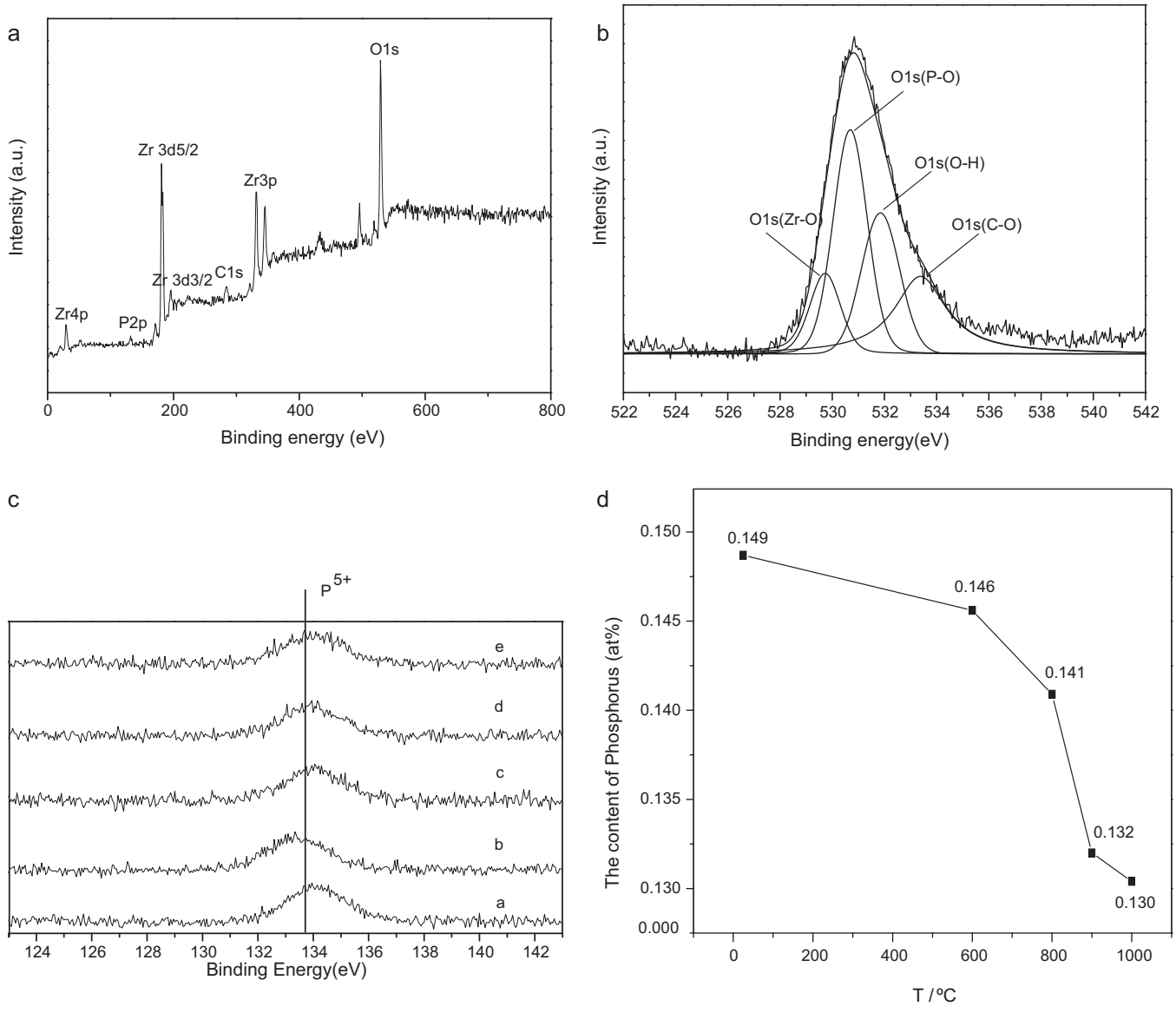

Fig. 9. (a) XPS spectrum of P-ZrO_2 calcined at 800 °C for 2 h; (b) XPS spectra of O 1s for P-ZrO_2 samples soaked in phosphate solution (0.5 M) and calcined at 800 °C. (c) XPS spectra of the P 2p region taken on the surface of the sample (a) P-ZrO_2 and (b–e) P-ZrO_2 calcined at 600, 800, 900, and 1000 °C respectively. (d) The content of phosphorus on the surface of P-ZrO_2 samples calcined at different temperatures.

of phosphate can be represented schematically in Fig. 10. The possible mechanism could be explained as follows. P species can occupy the surface of ZrO_2 particles by adsorption. The P species absorbed on the surface of ZrO_2 particles play a key role in the grain growth. The P species can reduce the grain boundary mobility and energy which are the crucial factors for improving the thermal stability of nanosized particles [14]. On the other hand, the P species on the surface of ZrO_2 prevent direct contact of particles due to steric effect and deactivate the defect sites of ZrO_2 which play a key role in the grain growth [15]. Hence, the grain growth of ZrO_2 can be effectively hindered.

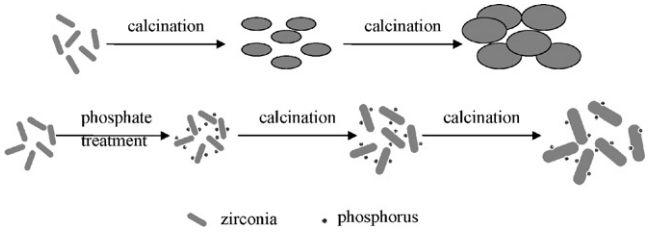

Fig. 10. Schematic illustration of the effect of phosphorus species on the grain growth of ZrO_2.

4. Conclusions

In summary, we have demonstrated a simple and facile method for inhibiting the grain growth of nanosized ZrO_2 when the particles were calcined at high temperatures. The as-prepared ZrO_2 powders were soaked in the phosphate solution with different concentrations for 24 h. The experimental results show that the untreated ZrO_2 grow and agglomerate to bulk seriously with the increasing calcination temperatures, while

the ZrO_2 crystal treated with phosphate solution remains nanosized particles when the powders were calcined at high temperatures. It can be concluded that phosphate treatment played an important role in inhibiting the crystal grain growth of ZrO_2. The possible mechanism could be explained that the phosphate ions on the surface of zirconia reduce the grain boundary mobility and energy, deactivate the defect sites and prevent direct contact of particles due to steric effect. This simple method could be extended to other metal oxide to enlighten the use of nanoparticles in ceramics field. Further investigation of the inhibition function of phosphate on the grain growth of other nanosized metal oxides was underway.

Acknowledgment

This work was supported by the Nature Science Foundation of Hebei Province (Grant No. B2010000360).

References

[1] X.L. Wang, L.C. Guo, Effect of temperature on the stability of aqueous ZrO_2 suspensions, Colloid Surf. A: Physicochem. Eng. Aspects 304 (2007) 1–6.
[2] L.R. Li, W.Z. Wang, Synthesis and characterization of monoclinic ZrO_2 nanorods by a novel and simple precursor thermal decomposition approach, Solid State Commun. 127 (2003) 639–643.
[3] C.W. Chen, X.S. Yang, A.S.T. Chiang, An aqueous process for the production of fully dispersible t-ZrO_2 nanocrystals, J. Taiwan Inst. Chem. Eng. 40 (2009) 296–301.
[4] V. Grover, R. Shukla, A.K. Tyagi, Facile synthesis of ZrO_2 powders: control of morphology, Scripta Mater. 57 (2007) 699–702.
[5] K.G. Kanade, J.O. Baeg, S.K. Apte, T.L. Prakash, B.B. Kale, Synthesis and characterization of nanocrystallined zirconia by hydrothermal method, Mater. Res. Bull. 43 (2008) 723–729.
[6] Y.H. Rong, Q.P. Meng, Y.L. Zhang, T.Y. Hsu, Phase stability and its intrinsic conditions in nanocrystalline materials, Mater. Sci. Eng. 438 (2006) 414–419.
[7] M. Ghiaci, H. Aghaei, A. Abbaspur, Size-controlled synthesis of ZrO_2–TiO_2 nanoparticles prepared via reverse micelle method: investigation of particle size effect on the catalytic performance in vapor phase Beckmann rearrangement, Mater. Res. Bull. 43 (2008) 1255–1262.
[8] W. Li, L. Gao, Compacting and sintering behavior of nano ZrO_2 powders, Scripta Mater. 44 (2001) 2269–2272.
[9] G.H. Du, Q. Chen, W. Zhou, G. Du, L.M. Peng, Exfoliating $KTiNbO_5$ particles into nanosheets, Chem. Phys. Lett. 377 (2003) 445–448.
[10] A.M. Peiro, J. Peral, C. Domingo, X. Domenech, J.A. Ayllon, Low-temperature deposition of TiO_2 thin films with photocatalytic activity from colloidal anatase aqueous solutions, Chem. Mater. 13 (2001) 2567–2573.
[11] L. Kőrösi, S. Papp, V. Meynen, P. Cool, E.F. Vansant, I. Dékány, Preparation and characterization of SnO_2 nanoparticles of enhanced thermal stability: the effect of phosphoric acid treatment on $SnO_2{\cdot}nH_2O$, Colloid Surf. A: Physicochem. Eng. Aspects 268 (2005) 147–154.
[12] J.C. Yu, L.Z. Zhang, Z. Zheng, J.C. Zhao, Synthesis and characterization of phosphated mesoporous titanium dioxide with high photocatalytic activity, Chem. Mater. 15 (2003) 2280–2286.
[13] P.K. Pattnayak, K.M. Parida, Studies on PO_4^{3-}/ZrO_2: II. Effect of H_3PO_4 on textual and acidic properties of ZrO_2, J. Colloid Interface Sci. 226 (2000) 340–345.
[14] X.H. Feng, J.Z. Liu, P. Li, Y.F. Zhang, Y. Wei, The inhibition effect of phosphate on crystal grain growth of nanosized titania, Rare Met. 28 (2009) 385–390.
[15] C.C. Wang, J.B. Li, Y.F. Zhang, Y. Wei, J.Z. Liu, The influence of phosphate on crystal grain growth of nanosized SnO_2, J. Alloy Compd. 493 (2010) 64–69.
[16] G.Q. Xu, Z.X. Zheng, Y.C. Wu, N. Feng, Effect of silica on the microstructure and photocatalytic properties of titania, Ceram. Int. 35 (2009) 1–5.
[17] A. Bhaumik, S. Inagaki, Mesoporous titanium phosphate molecular sieves with ion-exchange capacity, J. Am. Chem. Soc. 123 (2001) 691–696.
[18] W.Q. Gong, A real time in situ ATR–FTIR spectroscopic study of linear phosphate adsorption on titania surfaces, Int. J. Miner. Process. 63 (2001) 147–165.
[19] M.S. Niasari, M. Dadkhah, F. Davar, Synthesis and characterization of pure cubic zirconium oxide nanocrystals by decomposition of bis-aqua, tris-acetylacetonato zirconium (IV) nitrate as new precursor complex, Inorg. Chim. Acta 362 (2009) 3969–3974.
[20] S. Baunack, S. Oswald, D. Scharnweber, Depth distribution and bonding states of phosphorus implanted in titanium investigated by AES, XPS and SIMS, Surf. Interface Anal. 26 (1998) 471–479.
[21] S.J. Splinter, R. Rofagha, N.S. Mcintyre, U. Erb, XPS characterization of the corrosion films formed on nanocrystalline Ni–P alloys in sulphuric acid, Surf. Interface Anal. 24 (1996) 181–186.